PALEOCEANOGRAPHY, VOL. 25, PA2208, doi:10.1029/2009PA001780, 2010

Late Pliocene equatorial Pacific

Martín Medina-Elizalde[1,2] and David W. Lea[3]

Received 13 April 2009; revised 8 December 2009; accepted 22 December 2009; published 28 May 2010.

[1] Late Pliocene foraminiferal Mg/Ca and $\delta^{18}O$ records from Ocean Drilling Program Hole 806B in the western equatorial Pacific (WEP) reveal warm pool climate evolution during the onset of Northern Hemisphere glaciation, 3.1–2.3 Myr B.P. Mg/Ca data indicate an average late Pliocene sea surface temperature (SST) of 27.8°C, a small long-term cooling of 0.3°C between 3.1 and 2.3 Ma, and a glacial-interglacial (G-I) SST range of 2°C throughout this time interval. For comparison, Pleistocene SSTs at this site over the last 0.9 Myr average 27.7°C with a G-I range of 3°C. Orbital-scale variability in Hole 806B SSTs during the late Pliocene occurs predominantly at ~100 ka, in contrast to foraminiferal $\delta^{18}O$ records, which show a dominant 41 kyr period. Variability at a 41 kyr period, out of phase with local annual insolation changes driven by obliquity, is also observed in the new WEP SST record. The WEP SST record suggests that an ~3°C equatorial Pacific SST zonal gradient prevailed during the late Pliocene, compatible with a weaker Walker circulation. Adjustment of Hole 806B SSTs for past changes in seawater Mg/Ca suggests that SSTs higher than 30°C prevailed at 3 Myr B.P., followed by a progressive cooling of the warm pool through the late Pliocene. The characteristics of late Pliocene tropical climate evolution suggest that atmospheric greenhouse gas forcing played a major role in driving the observed G-I SST changes.

Citation: Medina-Elizalde, M., and D. W. Lea (2010), Late Pliocene equatorial Pacific, *Paleoceanography*, *25*, PA2208, doi:10.1029/2009PA001780.

1. Introduction

[2] During the late Pliocene (3.6–1.8 Ma), the climate of the Earth transitioned from a state of general global warmth to one of significant continental glaciation in the Northern Hemisphere. A progressive positive shift in foraminiferal $\delta^{18}O$ records, together with evidence of major deposition of ice-rafted detritus in the North Atlantic and North Pacific, indicates massive accumulation of ice, predominantly on the Northern Hemisphere continents between 3.1 and 2 Ma [*Jansen et al.*, 1988; *Lisiecki and Raymo*, 2005; *Raymo et al.*, 1989; *Shackleton et al.*, 1984]. Late Pliocene foraminiferal oxygen isotope records suggest that high-latitude Northern Hemisphere glaciation and/or deep ocean temperature cycles had a dominant periodicity of 41 kyr and that the dominant ~100 kyr period did not appear until after the mid-Pleistocene climate transition (MPT), at ~1 Ma [*Berger et al.*, 1999].

[3] There has been considerable effort devoted to determining the magnitude of Pliocene tropical Pacific warmth and the climatic factors that maintained it [e.g., *Barreiro et al.*, 2006; *Brierley et al.*, 2009; *Haywood and Valdes*, 2004; *Ravelo et al.*, 2004, 2006; *Raymo et al.*, 1996; *Rickaby and Halloran*, 2005]. Significantly less attention has been devoted to characterizing tropical Pacific sea surface temperature (SST) cycles on glacial-interglacial (G-I) timescales and determining the driving factors of this variability [*Brierley et al.*, 2009; *Fedorov et al.*, 2006; *Groeneveld et al.*, 2006; *Lawrence et al.*, 2006].

[4] The only Pliocene-Pleistocene SST record available from the equatorial Pacific cold tongue with sufficient resolution to study G-I climate variability is the Ocean Drilling Program (ODP) Hole 846 (3°5′S, 90°49′W) record based on the alkenone unsaturation index [*Lawrence et al.*, 2006]. Three other equatorial Pacific SST records that extend back to the early Pliocene, one from the warm pool and the other two from the cold tongue [*Wara et al.*, 2005; *Dekens et al.*, 2007], have insufficient resolution (sampled every 1–40 kyr) and continuity (numerous sampling gaps from 15 to 40 kyr) to be well suited for studies on G-I scales.

[5] The Pliocene SST record from the eastern equatorial Pacific (EEP) cold tongue, ODP Hole 846, shows dominant variability at a 41 kyr period with a phase consistent with high-latitude obliquity; that is, cold tongue SSTs are warm when annual insolation at the poles is at a maximum (and equatorial insolation is at a minimum) [*Lawrence et al.*, 2006]. Several studies have proposed that Pliocene-Pleistocene tropical variability in the obliquity band was driven by high-latitude annual insolation changes and/or changes in meridional insolation gradients [*Fedorov et al.*, 2006; *Lawrence et al.*, 2006; *Liu and Herbert*, 2004; *Philander and Fedorov*, 2003; *Raymo and Nisancioglu*, 2003]. According to these studies, obliquity controls tropical SST variability by influencing the depth of the EEP thermocline, which oscillates to sustain a cycle of Pacific Ocean heat transport [*Philander and Fedorov*, 2003] or as a

[1]Department of Geosciences, University of Massachusetts Amherst, Amherst, Massachusetts, USA.
[2]University Corporation for Atmospheric Research, Boulder, Colorado, USA.
[3]Department of Earth Science, University of California, Santa Barbara, California, USA.

0883-8305/10/2009PA001780

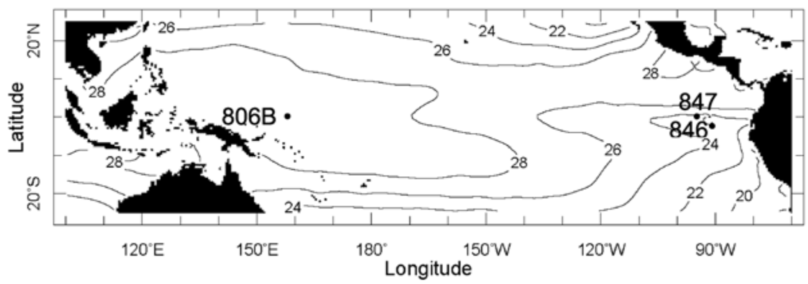

Figure 1. Eastern and western Pacific Ocean Drilling Program (ODP) site locations: western equatorial Pacific (WEP) warm pool ODP Hole 806B (0°19.1′N, 159°21.7′E; 2520 m water depth), eastern equatorial Pacific (EEP) cold tongue ODP Hole 847 (0°N, 95°W; 3373 m water depth) [*Wara et al.*, 2005], and EEP cold tongue ODP Hole 846 (3°5′S, 90°49′W; 3296 m water depth) [*Lawrence et al.*, 2006; *Wara et al.*, 2005]. Mean annual SSTs are available at http://iridl.ldeo.columbia.edu/SOURCES/.NOAA/.NODC/.WOA98/.

response to meridional insolation gradients [*Raymo and Nisancioglu*, 2003]. A corollary of these hypotheses is the prediction of a significantly larger G-I SST response in the EEP region, as opposed to the warm pool, because the thermocline is shallow enough for the trade winds to drive SSTs by modulating upwelling [*Fedorov et al.*, 2006; *Lawrence et al.*, 2006; *Liu and Herbert*, 2004; *Philander and Fedorov*, 2003; *Raymo and Nisancioglu*, 2003]. As pointed out by *Medina-Elizalde and Lea* [2005], however, the warm pool should not be affected by the thermocline shoaling mechanism because the thermocline is too deep to affect surface temperatures in this region. Furthermore, in the warm pool, SST is primarily determined through a one-dimensional balance between heat storage and heat flux to the atmosphere [*Clement et al.*, 1996; *Pierrehumbert*, 2000; *Seager et al.*, 1988].

[6] Consideration of the controls on SSTs in the cold tongue and warm pool can be used as a diagnostic tool to identify potential driving mechanisms of G-I SST cycles, particularly, to distinguish between atmospheric and oceanographic forcings. *Medina-Elizalde and Lea* [2005] showed that the evolution of equatorial Pacific SSTs during the Pleistocene was characterized by similar and synchronous SST cycles in the warm pool and cold tongue regions, with SST changes preceding high-latitude glaciations by several thousand years [*Liu and Herbert*, 2004; *Medina-Elizalde and Lea*, 2005]. This pattern, which is inconsistent with a larger SST response of the EEP cold tongue as expected from a mechanism involving adjustment of the EEP thermocline, was interpreted to reflect a major control by atmospheric greenhouse gases, particularly from CO_2, and their associated feedbacks [*Medina-Elizalde and Lea*, 2005].

[7] Here we present high-resolution equatorial Pacific Mg/Ca-based temperature, $\delta^{18}O$, and $\delta^{18}O$ seawater histories available for the late Pliocene. These records were derived from ODP Hole 806B, a site on the equator in the heart of the Pacific warm pool that shows constant sedimentation rates and excellent foraminiferal preservation. This site has already yielded benchmark Pleistocene and Pliocene records [*Berger et al.*, 1993; *Lea et al.*, 2000; *Medina-Elizalde and Lea*, 2005; *Wara et al.*, 2005].

[8] Time series analysis of the new late Pliocene Hole 806B SST record reveals previously unreported G-I SST variability that contrasts with records from high-latitude climate and challenges the conventional view of the late Pliocene "41 kyr world." Furthermore, the new Hole 806B SST record provides evidence that reveals the possible mechanism driving equatorial Pacific SST variability. We discuss our results in the context of three major hypotheses proposed to explain G-I variability in equatorial Pacific SSTs: the thermocline, thermostat, and greenhouse forcing hypotheses. The evidence from the available tropical Pacific paleoclimate records indicates that forcing by atmospheric greenhouse gases played a major role in driving late Pliocene equatorial Pacific G-I SSTs.

2. Methods

[9] We measured Mg/Ca and $\delta^{18}O$ in tests (shells) of the surface-dwelling planktonic foraminifer *Globigerinoides ruber* from sediment core ODP Hole 806B on the Ontong Java Plateau (OJP) (0°19.1′N, 159°21.7′E; 2520 m water depth) (Figure 1). We converted *G. ruber* Mg/Ca data to annual SSTs using a relationship based on Pacific sediment core top analyses by *Lea et al.* [2000]. The $\delta^{18}O$ seawater ($\delta^{18}O$ water) record was calculated by removing the component in planktonic $\delta^{18}O$ due to temperature using Mg/Ca-derived SSTs and the low-light paleotemperature equation determined for *Orbulina universa* [*Bemis et al.*, 1998].

[10] Cores 6H-5W through 8H-5W from Hole 806B were sampled at 5 cm intervals. Approximately 70–90 *G. ruber* shells were picked from the 250–350 μm–size fraction of each sample interval. Shells were gently crushed, homogenized, and split into three aliquots with ratios of approximately 2:2:1. The first two of these aliquots were cleaned using the University of California, Santa Barbara standard foraminiferal cleaning procedure [*Lea et al.*, 2000]. Dissolved samples were analyzed by the isotope dilution/internal standard method using a Thermo Scientific Finnigan Element 2 sector field inductively coupled plasma–mass spectrometer. The third (smaller) aliquot was used to analyze stable isotope composition using a GV Instruments IsoPrime isotope ratio mass spectrometer. Analytical reproducibility of Mg

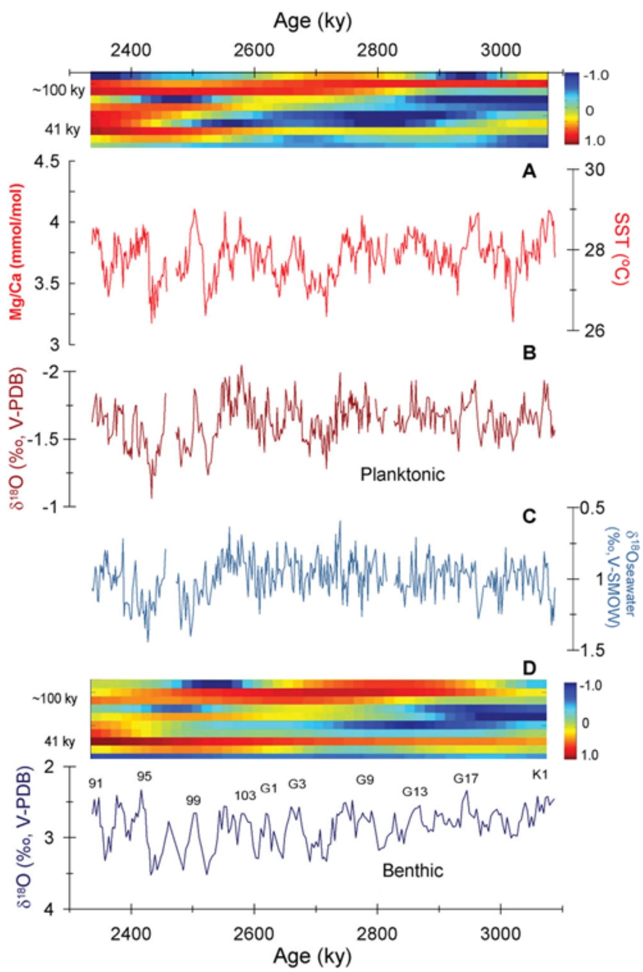

Figure 2. Late Pliocene WEP ODP Hole 806B (0°19.1′N, 159°21.7′E; 2520 m water depth) records based on the surface-dwelling foraminifera *G. ruber*. Gaps in the record are a result of coring gaps. The chronology is based on wiggle matching to the target benthic foraminiferal δ^{18}O stack by *Lisiecki and Raymo* [2005]. (a) *G. ruber* Mg/Ca-derived SST record. Mg/Ca data were converted using the relationship $(Mg/Ca)_{foram} = 0.3 \exp(0.089\ SST)$, where SST is in °C [*Lea et al.*, 2000]. Each point is an average of two to four replicates. The *G. ruber* SST record shows a modest 0.3°C long-term trend over the late Pliocene. (b) *G. ruber* δ^{18}O record and (c) δ^{18}O seawater record, calculated by extracting the component in planktonic δ^{18}O explained by the Mg/Ca SSTs. (d) Benthic *C. wuellerstorfi* foraminiferal δ^{18}O record [*Karas et al.*, 2009] showing a long-term positive shift equivalent to 0.38‰/Myr. Some marine isotopic stages are indicated. Evolutionary spectral analyses for the SST record (Figure 2a) and benthic foraminiferal δ^{18}O record (Figure 2d) are based on a multitaper method with 200 kyr windows and 50 kyr "jumps." The ODP Hole 806B SST record and benthic and planktonic foraminiferal δ^{18}O records are spectrally similar, with significant coherent amplitude at 41 and ~100 kyr periods. The SST record, however, has a greater contribution from the ~100 kyr period, whereas the 41 kyr period is dominant in both foraminiferal δ^{18}O records.

determinations was ±0.7% (1 standard deviation), and the average reproducibility of Mg/Ca sample splits was ±0.08 mmol/mol, equivalent to ±2.2% or ~0.2°C. The error of SST estimations related to G-I calcite preservation changes is ~0.5°C based on the similar lysocline history between the Pliocene and Pleistocene suggested by $CaCO_3$ preservation records [*Farrell and Prell*, 1991; *Lea et al.*, 2000]. The analytical precision of the δ^{18}O measurements is better than ±0.06%, as determined by replicate analysis of National Bureau of Standards (NBS) 19 and a second Carrara marble laboratory standard. Elemental ratios of Mn/Ca, Fe/Ca, and Al/Ca were analyzed at the same time as Mg/Ca to assess cleaning efficacy. There were no correlations between these elements and Mg/Ca throughout the sequence.

[11] The records span the late Pliocene between 3.1 and 2.3 Myr B.P., encompassing marine oxygen isotope stages (MISs) K1 to 91, with a resolution of 1.7 ± 0.3 kyr (Figure 2). We constructed the ODP Hole 806B age model by tuning a Hole 806B benthic (*Cibicidoides wuellerstorfi*) foraminiferal δ^{18}O record (10 cm sampling resolution [*Karas et al.*, 2009]) to the LR04 foraminiferal δ^{18}O stack [*Lisiecki and Raymo*, 2005] by graphical correlation of stage transitions using the AnalySeries 1.2 software [*Paillard et al.*, 1996]. The LR04 δ^{18}O stack integrates up to 25 records from globally distributed sites over the time interval between 2 and 3.1 Ma.

[12] The cross correlation between the Hole 806B *C. wuellerstorfi* δ^{18}O record and the LR04 δ^{18}O stack is r = 0.83 (cross correlations are calculated using the Arand software [*Howell et al.*, 2006]). Hole 806B has remarkably constant sedimentation rates (2.8 ± 0.3 cm/kyr) between 2.3 and 3.1 Ma, and because it lies above the present-day lysocline depth, it also has moderately good preservation of foraminiferal shells. There are two core gaps of ~22 cm (~8 kyr) that include parts of MIS 97 and MIS G11. The Hole 806B benthic foraminiferal δ^{18}O record is spectrally similar to the LR04 stack reference record, with characteristic dominance of 41 kyr and a weaker contribution at ~100 and 23 kyr periods.

3. Results

[13] The Hole 806B *G. ruber* δ^{18}O and Mg/Ca-derived SST data indicate 20 G-I oscillations from MIS K1 to MIS 91 between 3.1 and 2.3 Ma (Figure 2). The *G. ruber* δ^{18}O record shows a modest 0.1‰ negative shift and a muted G-I range of 0.6‰ during this time interval. The late Pliocene *G. ruber* Mg/Ca range is ~1 mmol/mol (from 3.2 to 4.2 mmol/mol), with higher Mg/Ca values associated with interglacial intervals and lower Mg/Ca values associated with glacial intervals. Average SST is 27.8°C ± 0.5°C, and the glacial-interglacial SST range is 2°C (±2 standard deviations from the mean). The warmest SST observed, 29.2°C, corresponds to MIS 99, and the coldest, 26.4°C, corresponds to MIS 96. The SST record documents a small but statistically significant long-term cooling of 0.3°C/Myr over the late Pliocene. Tectonic backtracking of the OJP, where Site 806B is located, suggests a 1.3° southeasterly location with respect to its position 3 Myr ago [*Kroenke et al.*, 2004]. On the basis of the modern warm pool temperature field, no SST correction is needed to account for the migration of the OJP over the last 3 Myr.

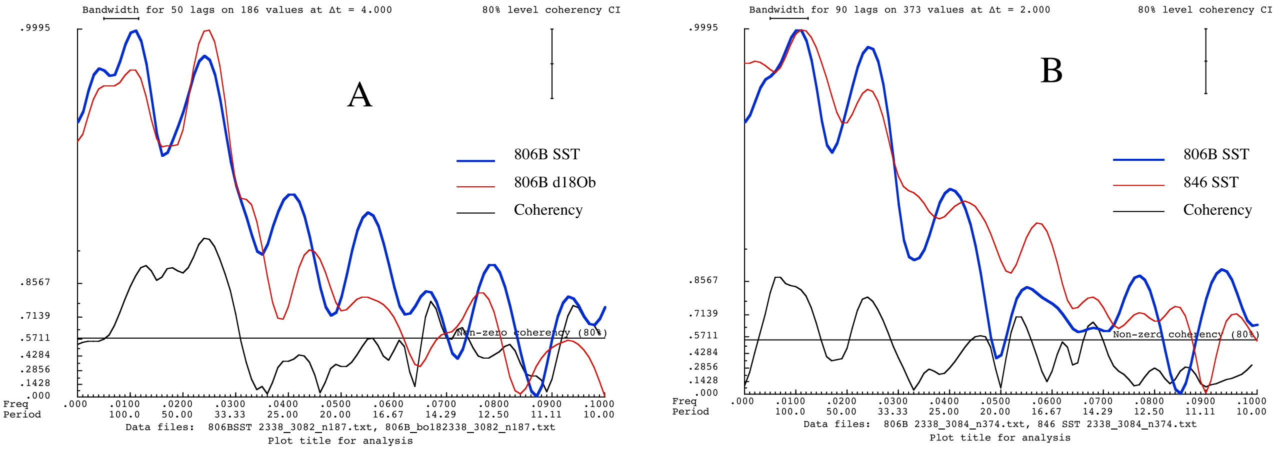

Figure 3. Cross-spectral analyses (a) between Hole 806B SST and benthic δ^{18}O and (b) between Hole 806B SST and ODP Hole 846 SST from 3084 to 2338 kyr B.P. The analyses demonstrate that 100 kyr power is higher in the SST record than the benthic δ^{18}O record (Figure 3a) and the SST record from ODP Hole 846 also has higher 100 kyr power (Figure 3b). The spectral density of the 100 and 41 kyr peaks in both records overlaps within error. The records have an overall cross correlation of 0.63 (Figure 3a) and 0.54 (Figure 3b) [*Howell et al.*, 2006].

[14] The Hole 806B δ^{18}O water record, which reflects continental ice volume and local salinity variability, does not indicate a statistically significant long-term trend (Figure 2d). The lack of a trend in δ^{18}O water contrasts with the positive long-term shift observed in the LR04 benthic foraminiferal δ^{18}O stack of 0.5‰/Myr over the late Pliocene. The observed δ^{18}O water G-I range is 0.5‰ during the late Pliocene, with more negative values characteristic of interglacial intervals and more positive values associated with glacial intervals. Spectrally, the δ^{18}O water record is characterized by a dominant 100 kyr period and minor contributions from the 23 and 41 kyr periods.

[15] The ODP Hole 806B SST record and benthic and planktonic foraminiferal δ^{18}O records are spectrally similar, with significant coherent amplitude at 41 and ~100 kyr periods (Figure 2). The SST record, however, has a slightly greater contribution from the ~100 kyr period relative to the 41 kyr period, with amplitudes of 0.34°C and 0.29°C, respectively, whereas the 41 kyr period is the stronger period in the benthic foraminiferal δ^{18}O record, with amplitudes of 0.17‰ and 0.13‰ at 41 and 100 ka, respectively (the spectral density of both peaks in the two records overlaps within error) [*Howell et al.*, 2006] (Figures 2 and 3a). The ODP Hole 806B planktonic δ^{18}O record, in contrast to these two records, shows similar contributions at 100 and 41 kyr periods, with an amplitude of 0.07‰ in each. The cross correlation between the Hole 806B SST and benthic δ^{18}O records is higher (r = 0.63) than that between the SST and *G. ruber* δ^{18}O records (r = 0.53). Cross-spectral analysis indicates that SST changes precede benthic δ^{18}O variability by 7.4 ± 3 kyr and 1.9 ± 0.9 kyr at the 100 and 41 kyr periods, respectively (95% confidence interval (CI)). Similarly, SSTs precede planktonic δ^{18}O by 11.5 ± 9 kyr and 2.5 ± 1 kyr at the 100 and 41 kyr periods, respectively. The Hole 806B benthic and planktonic foraminiferal δ^{18}O records are in phase at the dominant 41 and 100 kyr period components (r = 0.54).

[16] Comparison of late Pliocene Hole 806B SSTs with a previous study of Pleistocene SST evolution, also from Hole 806B [*Lea et al.*, 2000], indicates that the observed G-I SST range over the late Pliocene is smaller than that over the Pleistocene: 2°C versus 3.6°C (based on ±2 standard deviations from the mean) (Figure 4). Observed SST averages, however, are similar: 27.8°C over the late Pliocene and 27.7°C over the Pleistocene [*Lea et al.*, 2000; *Medina-Elizalde and Lea*, 2005]. The Hole 806B SST record between 1 Ma and the Holocene [*Lea et al.*, 2000; *Medina-Elizalde and Lea*, 2005] reveals a similar spectral pattern to the late Pliocene record, with a dominant 100 kyr component

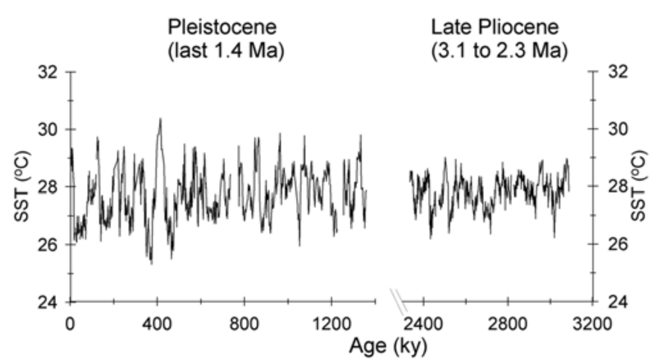

Figure 4. Pleistocene [*Lea et al.*, 2000; *Medina-Elizalde and Lea*, 2005] and late Pliocene (this study) Hole 806B western equatorial Pacific SST records based on *G. ruber* Mg/Ca. Mean SSTs for the two time intervals are 27.7°C and 27.8°C, respectively. The late Pliocene warm pool G-I SST range was ~1°C smaller than during the Pleistocene. The data indicate that, without adjustment for changes in seawater Mg/Ca, average Pleistocene and Pliocene SSTs were essentially identical.

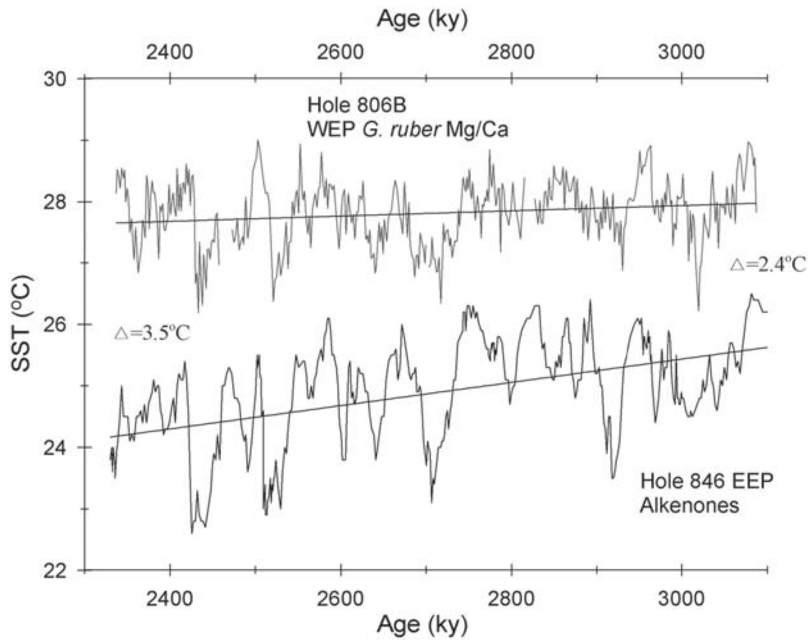

Figure 5. Late Pliocene western equatorial Pacific ODP Hole 806B SST record based on *G. ruber* Mg/Ca (this study, unadjusted for seawater changes) and eastern equatorial Pacific cold tongue ODP Hole 846 (3°5′S, 90°49′W; 3296 m water depth) SST record based on the alkenone unsaturation index [*Lawrence et al.*, 2006]. The warm pool and cold tongue records show similar and synchronous glacial-interglacial SST cycles, which precede oxygen isotope cycles by several thousand years. Trend comparisons between the cold tongue and warm pool records suggest that the equatorial Pacific zonal SST gradient increased from 2.4°C at 3.1 Ma to 3.5°C by 2.3 Myr before present.

and a weaker 41 kyr component, in addition to a similar phase lead over foraminiferal $\delta^{18}O$ records.

[17] An additional factor that must be considered in calculating absolute Pliocene SSTs from foraminiferal Mg/Ca is the potential influence of past changes in seawater Mg/Ca (Mg/Ca_{sw}). Available pore water data and modeling results [*Fantle and DePaolo*, 2006] suggest that Mg/Ca_{sw} between 3.1 and 2.3 Ma was about 20% below modern values. Compensating for this change requires an adjustment to Mg/Ca-based SSTs of about +1°C [*Medina-Elizalde et al.*, 2008]. This adjustment affects not the glacial-interglacial variability in SST but rather the absolute values and secular trends. For example, the adjustment increases the secular cooling between 3.1 and 2.3 Ma and also increases the Pacific zonal SST contrast during this time interval by ~1°C (see section 4). Adjustment to Mg/Ca-based Pliocene SSTs is probably required, but there is considerable uncertainty about the exact magnitude of past Mg/Ca_{sw} changes [*Fantle and DePaolo*, 2006] and whether the partition coefficient for foraminiferal Mg/Ca depends on Mg/Ca_{sw} [*Medina-Elizalde et al.*, 2008].

4. Discussion

4.1. Comparison Between Western and Eastern Equatorial Pacific SST Records: Pattern Matters

[18] Comparison between the new Hole 806B SST record and the published ODP Hole 846 SST record based on alkenone unsaturation, which has a comparable resolution (3°5′S, 90°49′W; 3296 m water depth [*Lawrence et al.*, 2006]) (Figure 1), suggests that G-I SST changes in the western equatorial Pacific (WEP) were somewhat smaller than in the EEP (Figure 5). The EEP cold tongue G-I SST range was ~3°C (detrended) during the late Pliocene, ~1°C larger than in the WEP warm pool. Time series analysis indicates that the SST ranges (twice the amplitude) associated with the ~100 and 41 kyr periods are 1.2°C and 0.75°C, respectively, in the Hole 846 SST record, whereas these ranges are 0.68°C and 0.58°C, respectively, in the Hole 806B SST record. It is important to point out that the dominant 100 kyr period present in the ODP Hole 846 SST record was not reported in the original study [*Lawrence et al.*, 2006] because this variability was removed from the record to stress the higher-frequency 41 kyr variability, which was the focus of the study [*Lawrence et al.*, 2006, Figure 2; K. Lawrence, Lafayette College, personal communication, 2008]. Cross-spectral comparison indicates that the Hole 806B and Hole 846 SST records are statistically coherent (95% CI), in phase, and that both have higher spectral density in the ~100 kyr period relative to the 41 kyr period (the spectral density of both peaks in the two records overlaps within error) (Figure 3b).

[19] Comparison of long-term trends between the WEP (Hole 806B Mg/Ca) and EEP (Hole 846 alkenone unsaturation) SST records indicates that the difference between average cold tongue and warm pool SSTs increased progressively from 2.4°C at 3.1 Ma to 3.5°C at 2.3 Ma (Figure 5). It is important to point out that Site 846, located on the Nazca

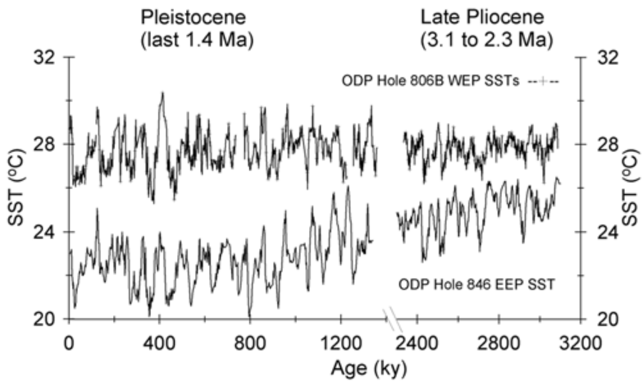

Figure 6. Pleistocene and late Pliocene Hole 806B western equatorial Pacific SST records based on *G. ruber* Mg/Ca (unadjusted for seawater changes) and eastern equatorial Pacific cold tongue ODP Hole 846 SST records based on the alkenone unsaturation index [*Liu and Herbert*, 2004; *Lawrence et al.*, 2006]. The late Pliocene warm pool and cold tongue G-I SST ranges are ~1°C smaller than during the Pleistocene. The cold tongue G-I SST range is typically larger than the warm pool region.

Plate, has been near its present latitudinal position for its entire history, and thus, a temperature backtrack correction is likely not required [*Pisias et al.*, 1995]. The enhancement of the equatorial Pacific zonal SST gradient by ~1°C is almost completely due to the 1.4°C cooling in the eastern equatorial Pacific [*Lawrence et al.*, 2006]. This observation confirms prior observations of an increase in the zonal SST gradient during this time span [*Wara et al.*, 2005] but with some differences. For example, comparison between the more sparsely sampled (~10–40 kyr) late Pliocene ODP Hole 806B WEP *Globigerinoides sacculifer* Mg/Ca SST record [*Wara et al.*, 2005] and the ODP Holes 846 and 847 EEP cold tongue SST records, based on the alkenone unsaturation index (Hole 846 [*Lawrence et al.*, 2006]) and *G. sacculifer* Mg/Ca (Hole 847 [*Wara et al.*, 2005]), respectively, suggests an average late Pliocene equatorial Pacific SST zonal gradient of 2°C (Hole 846) or an absent gradient (~0.6°C ± 1.5°C) during most of the late Pliocene (Hole 847). The different estimates of the SST gradient relate to resolution, proxy, and/or site differences. Regardless, all of the comparisons support a reduced SST gradient along the equator during the late Pliocene.

[20] The ODP Hole 806B and Hole 846 SST records show that equatorial Pacific SSTs during the late Pliocene followed a similar pattern to that characteristic of the last million years of Pleistocene (i.e., after the mid-Pleistocene transition at 950 kyr B.P., here denoted post-MPT). Glacial-interglacial SST variability in the eastern and western equatorial regions during the late Pliocene and post-MPT was dominated by two periodicities: a stronger 100 kyr period and a weaker 41 kyr period, with a cold tongue SST range always larger than the warm pool region. One clear difference between the Pliocene and post-MPT is that the G-I SST range in both the warm pool and cold tongue was smaller during the late Pliocene than during the post-MPT (Figure 6).

4.2. Can the Thermocline Hypothesis Explain the G-I Pattern of Tropical Pacific SSTs?

[21] Several studies have proposed that high-latitude annual insolation changes driven by obliquity could potentially control tropical Pacific SSTs by creating an "imbalance" in the oceanic heat budget that would have to be restored by a heat gain/loss from the EEP cold tongue [*Philander and Fedorov*, 2003; *Fedorov et al.*, 2006]. To maintain a balanced heat budget, an increase in oceanic heat loss in high latitudes during obliquity minima requires an increase in heat gain in low latitudes, which is accomplished by shoaling the tropical thermocline, thus producing cooling of tropical surface waters associated with glacial intervals. Conversely, a decrease in oceanic heat loss in high latitudes during obliquity maxima deepens the tropical thermocline, producing warming of surface waters associated with interglacial intervals [*Philander and Fedorov*, 2003; *Fedorov et al.*, 2006]. Alternatively, obliquity could also influence tropical Pacific SSTs by modulating meridional pressure gradients and, thus, trade wind intensity and upwelling in the EEP cold tongue [*Raymo and Nisancioglu*, 2003]. These mechanisms involving vertical adjustments of the EEP thermocline should cause a particular SST pattern across the equatorial Pacific: variability in SST at 41 kyr periods in phase with high-latitude obliquity forcing and a larger SST range in the cold tongue than in the warm pool. The larger cold tongue SST range is expected because the thermocline is much shallower in the EEP than in the warm pool, making cold tongue SSTs more sensitive to vertical adjustments of the thermocline. As an illustration of the different sensitivity of surface water SSTs between the cold tongue and the warm pool to the tilt of the thermocline, today, monthly SST anomalies in the EEP associated with El Niño/La Niña events are out of phase with similar anomalies in the warm pool.

[22] The late Pliocene ODP Hole 806B warm pool and Hole 846 eastern equatorial Pacific SST records do suggest a larger SST range in the cold tongue region than in the warm pool: 0.75°C for the cold tongue and 0.58°C for the warm pool, in agreement with the prediction from the thermocline hypothesis (Figure 5). The small difference between the SST ranges (<0.2°C), however, suggests that another mechanism besides a thermocline shift must be controlling equatorial Pacific SST variability. Furthermore, adjustments of the thermocline driven by obliquity fail to explain the dominant 100 kyr SST cycles in both equatorial Pacific records. It is important to note that the 100 kyr SST range is also larger in the cold tongue (1.2°C) than in the warm pool (0.68°C), suggesting that the larger cold tongue SST change associated with 41 kyr variability may not necessarily be indicative of a response to changes in the depth of the EEP thermocline [*Philander and Fedorov*, 2003; *Fedorov et al.*, 2006].

4.3. High-Latitude Control of Tropical G-I SST Variability?

[23] As pointed out previously [*Liu and Herbert*, 2004; *Medina-Elizalde and Lea*, 2005], direct annual insolation changes at the equator driven by obliquity variations are out of phase with 41 kyr variability in tropical SSTs and also cannot explain the dominant 100 kyr periodicity in late

Pliocene tropical Pacific SST records. Tropical SST variability also leads foraminiferal δ^{18}O cycles (which are predominantly controlled by ice volume and polar temperatures) by several thousand years, arguing against a simple mechanism whereby the high latitudes drive the tropics [*Lea et al.*, 2000; *Liu and Herbert*, 2004; *Medina-Elizalde and Lea*, 2005; *Lawrence et al.*, 2006; this study]. It is important to note, however, that lead-lag observations based on comparing Mg/Ca-derived and alkenone-derived SSTs to benthic foraminiferal δ^{18}O may be influenced by significant lags in the mixing of oxygen isotopes into the deep ocean, as suggested by new modeling studies [*Wunsch and Heimbach*, 2008]. Additional evidence against a high-latitude control on tropical SST evolution is provided by the lack of sensitivity of tropical Pacific SSTs to the very large Northern Hemisphere ice sheets during the Last Glacial Maximum, as suggested by general circulation models [*Broccoli*, 2000; *Broccoli and Manabe*, 1987]. Because late Pliocene Northern Hemisphere ice sheets were smaller compared to the Pleistocene, the size and the associated climate forcing potential of Pliocene ice sheets were likely to also have been reduced [*Maslin et al.*, 1998].

4.4. Role of Atmospheric Carbon Dioxide

[24] An alternative hypothesis to explain the observed SST variability is that variability in atmospheric carbon dioxide at 100 and 41 kyr periods, and its associated feedbacks, controlled the evolution of equatorial Pacific SSTs during the late Pliocene. This suggestion is primarily based on the observation that the evolutionary patterns of equatorial Pacific SSTs during the late Pliocene and late Pleistocene time intervals are remarkably similar [*Lea et al.*, 2000; *Liu and Herbert*, 2004; *Medina-Elizalde and Lea*, 2005; *Lawrence et al.*, 2006; this study]. A previous study showed that during the post-MPT, the evolution of equatorial Pacific SSTs, Antarctic air temperatures, and atmospheric CO_2 was characterized by dominant 100 kyr and weaker 41 kyr cycles, with these changes occurring synchronously, within timescale uncertainties [*De Garidel-Thoron et al.*, 2005; *Lea*, 2004; *Medina-Elizalde and Lea*, 2005].

[25] Recent climate model studies indicate that tropical Pacific SSTs, particularly the EEP cold tongue, are sensitive to the radiative effect of rising atmospheric CO_2 and its associated feedbacks [*Knutson and Manabe*, 1998; *Vecchi et al.*, 2008; *Vecchi and Soden*, 2007]. The stronger SST response of the EEP cold tongue predicted by these models results from a weakening of the Walker cell and therefore weaker EEP upwelling. In the warm pool region, on the other hand, where the thermocline is too deep to be significantly affected by changes in the strength of the Walker cell, SSTs are expected to rise at a slower rate [*Knutson and Manabe*, 1998; *Vecchi et al.*, 2008; *Vecchi and Soden*, 2007].

[26] If atmospheric CO_2 changes during the late Pliocene followed the phase of high-latitude obliquity, as was the case for atmospheric CO_2 during the last half million years [*Lea*, 2004; *Shackleton*, 2000], the radiative influence of CO_2 on equatorial SSTs could account for both the phase and the SST lead over benthic δ^{18}O. The 100 kyr variability in atmospheric CO_2, on the other hand, could have an origin in the Southern Hemisphere around Antarctica, set by the turnover time for carbonate ions in the ocean with respect to the CO_2-induced weathering of silicate rocks and the burial of $CaCO_3$ on the seafloor [*Toggweiler*, 2008].

[27] Given the 100 kyr dominance in SST, why is the 100 kyr period not also dominant in late Pliocene foraminiferal δ^{18}O records? Assuming that tropical SSTs respond to atmospheric CO_2 forcing, the smaller late Pliocene WEP warm pool G-I SST range compared to the post-MPT implies a smaller G-I atmospheric CO_2 range. We hypothesize that high-latitude climate was particularly sensitive to orbital forcing from obliquity variations during the Pliocene and the early Pleistocene [*Huybers and Tziperman*, 2008], perhaps because G-I variability in CO_2 was too weak to have had a large effect on ice sheets. This hypothesis would imply that a threshold was reached at the MPT, when G-I variability in atmospheric CO_2 was sufficiently large to have exerted a major control on high-latitude climate, perhaps in conjunction with climate feedbacks from the tropics.

4.5. Long-Term Thermal Stability of the Pacific Warm Pool During the Pliocene-Pleistocene

[28] The long-term evolution of the tropical Pacific can be described as a progressive transition from relatively homogenous SSTs across the equatorial Pacific, reflecting either a perennial El Niño state, referred to as El Padre [*Molnar and Cane*, 2002; *Ravelo et al.*, 2004; *Wara et al.*, 2005], or more frequent El Niño events [*Haywood et al.*, 2007], to an SST distribution characterized by strong zonal gradients and a prominent EEP cold tongue [*Lea et al.*, 2000; *Wara et al.*, 2005; *Lawrence et al.*, 2006; this study]. This transition occurred over the late Pliocene, mostly in the form of progressive cooling in the cold tongue [*Wara et al.*, 2005; *Lawrence et al.*, 2006; this study]. WEP warm pool SSTs remained relatively stable throughout the last 5 Myr, as previously suggested by *Wara et al.* [2005] and confirmed by this study. The lack of a secular trend in warm pool SSTs during the late Pliocene is notable because Northern Hemisphere glaciation intensified over this time interval [*Jansen and Sjøholm*, 1991; *Shackleton et al.*, 1984], suggesting that the climate evolution of the WEP was decoupled from intensification of Northern Hemisphere glaciation. The long-term stability of the warm pool is also at odds with the notion that greenhouse gases, particularly CO_2 [*Haywood et al.*, 2005; *Lunt et al.*, 2008], and water vapor [*Brierley et al.*, 2009] were responsible for the gradual global cooling of the Pliocene and represents a paradox in light of general circulation model (GCM) results of Pliocene global climate, which appear to require higher greenhouse gas levels to explain Pliocene warmth [*Fedorov et al.*, 2006; *Haywood and Valdes*, 2004; *Haywood et al.*, 2007].

[29] One hypothesis to explain why warm pool SSTs were not warmer during the early Pliocene calls on specific atmosphere-ocean interactions that act as a "thermostat," preventing SSTs from rising above a certain limit. *Newell* [1979] and *Hartmann and Michelsen* [1993] argued that above 30°C–31°C, evaporative cooling would exceed the heat input from radiation, thus limiting any further rise of tropical SSTs. The models in support of this idea, however, lack interactive dynamical transports of heat in the ocean and the atmosphere. Recent studies based on fully coupled

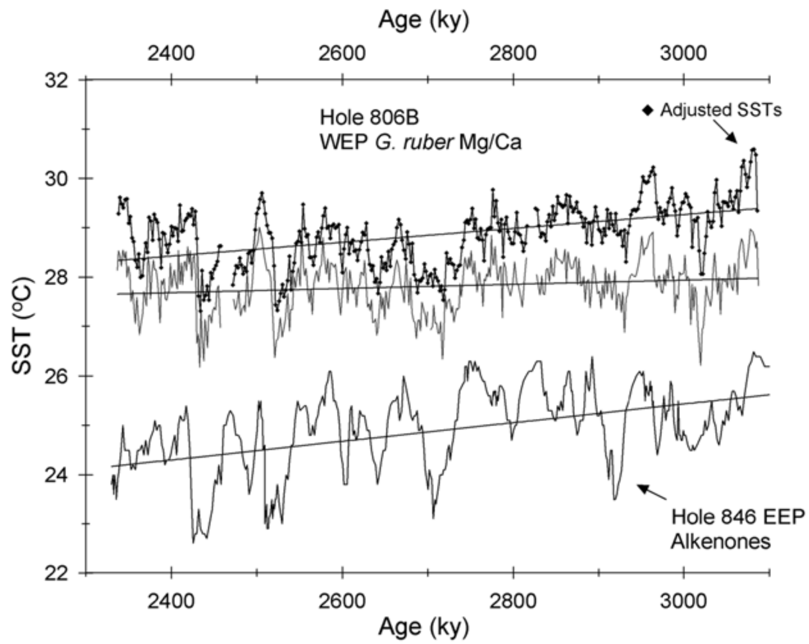

Figure 7. Late Pliocene western equatorial Pacific ODP Hole 806B SST records (this study) based on adjusted and unadjusted foraminiferal Mg/Ca and eastern equatorial Pacific cold tongue ODP Hole 846 SST record based on the alkenone unsaturation index [*Lawrence et al.*, 2006]. The adjusted SST record accounts for past variations in seawater Mg/Ca changes [*Medina-Elizalde et al.*, 2008]. Over the late Pliocene, the adjusted SST record indicates an ~1°C long-term cooling of the warm pool and 1°C warmer absolute SSTs than the unadjusted SST record. Trend comparisons between the cold tongue and warm pool (unadjusted) records are indicated in the plot. Trends between the cold tongue and the warm pool regions, calculated using the warm pool adjusted SST record, suggest that the zonal gradient increased from 3.8°C to 4.2°C during the late Pliocene.

ocean-atmosphere GCMs suggest, in contrast to the thermostat hypothesis, that warm pool SSTs could indeed rise above 31°C if, for instance, the concentration of atmospheric CO_2 rose above present levels of 375 ppm [*Haywood et al.*, 2005, 2007; *Vecchi et al.*, 2008]. If the results from these refined models are correct, why were warm pool SSTs not warmer during the early Pliocene warm interval?

[30] One possible answer might lie in a proxy bias that affects warm pool SSTs. The computation of SSTs from foraminiferal Mg/Ca assumes that the seawater Mg/Ca ratio has remained the same over the last 5 Myr [*Medina-Elizalde et al.*, 2008]. Recent studies based on pore water analysis and modeling suggest, however, that the seawater Mg/Ca ratio was ~20% lower during the late Pliocene [*Fantle and DePaolo*, 2006]. Available warm pool Pliocene SST records are based on the foraminiferal Mg/Ca technique because the alkenone unsaturation index, another SST proxy, saturates at temperatures higher than 27.5°C [*Conte et al.*, 2006; *Herbert*, 2003]. Adjustment of the Hole 806B Mg/Ca SST record to account for past changes in seawater Mg/Ca suggests that the warm pool was 1°C warmer during the late Pliocene than during the mid-Holocene, in agreement with recent climate model studies [*Haywood et al.*, 2007] (Figure 7). If this result is correct, it solves the paradox of unchanged Pliocene warm pool SSTs. The adjustment for changing seawater Mg/Ca suggested by *Medina-Elizalde et al.* [2008], however, has uncertainties and requires additional validation before it can be reliably incorporated into Pliocene proxy records.

4.6. Pacific Warm Pool Hydrological Evolution During the Late Pliocene

[31] The ODP Hole 806B $\delta^{18}O$ water record provides an additional way to evaluate Pliocene climatic trends in the equatorial Pacific (Figure 2c). To be placed in context, the $\delta^{18}O$ water record has to be compared to the global oxygen isotope trend, which records a 0.5‰/Myr increase over the late Pliocene, thought to reflect the growth of continental ice mass [*Lisiecki and Raymo*, 2005]. That the Hole 806B $\delta^{18}O$ water record displays no trend over this time interval suggests that western equatorial Pacific waters became more isotopically depleted, which, in turn, implies a long-term freshening. This freshening, in conjunction with an increased zonal SST gradient, is consistent with a strengthening of Walker circulation over the course of the late Pliocene (Figures 2c and 5) [*Ravelo et al.*, 2004; *Wara et al.*, 2005]. Additional support for this view is provided by the marked rise in EEP productivity documented by the Hole 846 productivity record [*Lawrence et al.*, 2006] because a stronger Walker circulation would enhance EEP upwelling and productivity. Adjustment of SSTs for changes in seawater Mg/Ca also affects the $\delta^{18}O$ water trend. The adjusted $\delta^{18}O$ water record, calculated by removing the component in planktonic $\delta^{18}O$ due to adjusted

SSTs, suggests a decreasing trend of 0.2‰ from 3.1 to 2.3 Ma, which would imply an even stronger progressive freshening of the warm pool during the late Pliocene.

5. Conclusions

[32] A late Pliocene (3.1–2.3 Myr B.P.) western equatorial Pacific (WEP) Mg/Ca-based SST record from ODP Hole 806B reveals previously unreported variability in tropical warm pool waters. The glacial-interglacial SST range over the late Pliocene is smaller than during the Pleistocene [*Lea et al.*, 2000], 2°C versus 3°C, and SST cycles are dominated by an ~100 kyr period and a weaker 41 kyr period that is out of phase with local annual insolation changes driven by obliquity. High-latitude climate records based on foraminiferal δ^{18}O, in contrast, are dominated by variability at 41 ka during the late Pliocene [*Lisiecki and Raymo*, 2005]. WEP warm pool SST cycles lead benthic δ^{18}O cycles by 7.4 ± 3 kyr and 1.9 ± 0.9 kyr at the 100 and 41 kyr periods. Comparison of the ODP Hole 806B SST record to an eastern equatorial Pacific cold tongue record based on alkenone unsaturation ratios [*Lawrence et al.*, 2006] suggests that the equatorial Pacific zonal SST gradient increased from 2.4°C at 3.1 Ma to 3.5°C at 2.3 Ma (estimated errors of ±1°C). These estimates of the late Pliocene zonal SST gradient are somewhat larger than in previous studies [*Wara et al.*, 2005]. The ODP Hole 806B δ^{18}O water record, computed from simultaneous Mg/Ca SSTs and δ^{18}O measurements, indicates a long-term freshening of the warm pool during the late Pliocene. The long-term trends in tropical SSTs and warm pool δ^{18}O water are both consistent with a strengthening of the Walker circulation during the late Pliocene. The character of late Pliocene equatorial Pacific temperature evolution suggests that glacial-interglacial SST cycles were driven at least in part by radiative forcing due to atmospheric CO_2 variability at 100 and 41 kyr periods. If ODP Hole 806B SSTs are adjusted for past seawater Mg/Ca changes [*Medina-Elizalde et al.*, 2008], they suggest a 1°C cooling between 3.1 and 2.3 Myr B.P., with late Pliocene warm pool SSTs exceeding 30°C. Higher Pliocene warm pool SSTs and a secular cooling during the late Pliocene are both consistent with a progressive decrease in atmospheric CO_2 over the Pliocene-Pleistocene, as suggested by models that attempt to simulate Pliocene warmth.

[33] **Acknowledgments.** This work was supported by U.S. NSF OCE502609. Additional support was provided by CONACYT-UCMEXUS. We thank G. Paradis for laboratory work at UCSB and P. Huybers for providing the code for the evolutionary spectral analysis. Reviews and comments by the Editor, G. Dickens, and an anonymous reviewer improved the manuscript.

References

Barreiro, M., et al. (2006), Simulations of warm tropical conditions with application to middle Pliocene atmospheres, *Clim. Dyn.*, *26*, 349–365, doi:10.1007/s00382-005-0086-4.

Bemis, B. E., H. J. Spero, J. Bijma, and D. W. Lea (1998), Reevaluation of the oxygen isotopic composition of planktonic foraminifera: Experimental results and revised paleotemperature equations, *Paleoceanography*, *13*, 150–160, doi:10.1029/98PA00070.

Berger, A., et al. (1999), Modeling Northern Hemisphere ice volume over the last 3 Ma, *Quat. Sci. Rev.*, *18*, 1–11, doi:10.1016/S0277-3791(98)00033-X.

Berger, W. H., T. Bickert, H. Schmidt, and G. Wefer (1993), Quaternary oxygen isotope record of pelagic foraminifers: Site 806, Ontong Java Plateau, *Proc. Ocean Drill. Program Sci. Results*, *130*, 381–395.

Brierley, C. M., et al. (2009), Greatly expanded tropical warm pool and weakened Hadley circulation in the early Pliocene, *Science*, *323*, 1714–1718, doi:10.1126/science.1167625.

Broccoli, A. J. (2000), Tropical cooling at the Last Glacial Maximum: An atmosphere–mixed layer ocean model simulation, *J. Clim.*, *13*, 951–976, doi:10.1175/1520-0442(2000)013<0951:TCATLG>2.0.CO;2.

Broccoli, A. J., and S. Manabe (1987), The influence of continental ice, atmospheric CO_2, and land albedo on the climate of the Last Glacial Maximum, *Clim. Dyn.*, *1*, 87–89, doi:10.1007/BF01054478.

Clement, B. M., et al. (1996), An ocean dynamical thermostat, *J. Clim.*, *9*, 2190–2196, doi:10.1175/1520-0442(1996)009<2190:AODT>2.0.CO;2.

Conte, M. H., M.-A. Sicre, C. Rühlemann, J. C. Weber, S. Schulte, D. Schulz-Bull, and T. Blanz (2006), Global temperature calibration of the alkenone unsaturation index ($U^{K'}_{37}$) in surface waters and comparison with surface sediments, *Geochem. Geophys. Geosyst.*, *7*, Q02005, doi:10.1029/2005GC001054.

De Garidel-Thoron, T., et al. (2005), Stable sea surface temperatures in the western Pacific warm pool over the past 1.75 million years, *Nature*, *433*, 294–298, doi:10.1038/nature03189.

Dekens, P. S., A. C. Ravelo, and M. D. McCarthy (2007), Warm upwelling regions in the Pliocene warm period, *Paleoceanography*, *22*, PA3211, doi:10.1029/2006PA001394.

Fantle, M. S., and D. J. DePaolo (2006), Sr isotopes and pore fluid chemistry in carbonate sediment of the Ontong Java Plateau: Calcite recrystallization rates and evidence for a rapid rise in seawater Mg over the last 10 million years, *Geochim. Cosmochim. Acta*, *70*, 3883–3904, doi:10.1016/j.gca.2006.06.009.

Farrell, J. W., and W. L. Prell (1991), Pacific $CaCO^3$ preservation and δ^{18}O since 4 Ma: Paleoceanic and paleoclimatic implications, *Paleoceanography*, *6*, 485–498, doi:10.1029/91PA00877.

Fedorov, A. V., et al. (2006), The Pliocene paradox (mechanisms for a permanent El Niño), *Science*, *312*, 1485–1489, doi:10.1126/science.1122666.

Groeneveld, J., et al. (2006), Pliocene mixed-layer oceanography for Site 1241, using combined Mg/Ca and δ^{18}O analyses of *Globigerinoides sacculifer*, *Proc. Ocean Drill. Program Sci. Results*, *202*, 1–27, doi:10.2973/odp.proc.sr.202.209.2006.

Hartmann, D. L., and M. L. Michelsen (1993), Large-scale effects on the regulation of tropical sea surface temperature, *J. Clim.*, *6*, 2049–2062, doi:10.1175/1520-0442(1993)006<2049:LSEOTR>2.0.CO;2.

Haywood, A. M., and P. J. Valdes (2004), Modeling Pliocene warmth: Contribution of atmosphere, oceans and cryosphere, *Earth Planet. Sci. Lett.*, *218*, 363–377, doi:10.1016/S0012-821X(03)00685-X.

Haywood, A. M., P. Dekens, A. C. Ravelo, and M. Williams (2005), Warmer tropics during the mid-Pliocene?: Evidence from alkenone paleothermometry and a fully coupled ocean-atmosphere GCM, *Geochem. Geophys. Geosyst.*, *6*, Q03010, doi:10.1029/2004GC000799.

Haywood, A. M., P. J. Valdes, and V. L. Peck (2007), A permanent El Niño–like state during the Pliocene?, *Paleoceanography*, *22*, PA1213, doi:10.1029/2006PA001323.

Herbert, T. D. (2003), Alkenone paleotemperature determinations, in *Treatise on Geochemistry*, vol. 6, edited by H. D. Holland and K. K. Turekian, pp. 391–432, Elsevier, Amsterdam.

Howell, P., et al. (2006), Arand time series analysis software, Brown Univ., Providence, R. I.

Huybers, P., and E. Tziperman (2008), Integrated summer insolation forcing and 40,000-year glacial cycles: The perspective from an ice-sheet/energy-balance model, *Paleoceanography*, *23*, PA1208, doi:10.1029/2007PA001463.

Jansen, E., and J. Sjøholm (1991), Reconstruction of glaciation over the past 6 Myr from ice-borne deposits in the Norwegian Sea, *Nature*, *349*, 600–603, doi:10.1038/349600a0.

Jansen, E., U. Bleil, R. Henrich, L. Kringstad, and B. Slettemark (1988), Paleoenvironmental changes in the Norwegian Sea and the northeast Atlantic during the last 2.8 m.y.: Deep Sea Drilling Project/Ocean Drilling Program sites 610, 642, 643, and 644, *Paleoceanography*, *3*, 563–581, doi:10.1029/PA003i005p00563.

Karas, C., et al. (2009), Mid-Pliocene climate change amplified by a switch in Indonesian subsurface throughflow, *Nat. Geosci.*, *2*, 434–438, doi:10.1038/ngeo520.

Knutson, T. R., and S. Manabe (1998), Model assessment of decadal variability and trends in the tropical Pacific Ocean, *J. Clim.*, *11*, 2273–2296, doi:10.1175/1520-0442(1998)011<2273:MAODVA>2.0.CO;2.

Kroenke, L. W., P. Wessel, and A. Sterling (2004), Motion of the Ontong Java Plateau in the hot-spot frame of reference: 122 Ma–present, *Geol. Soc. Spec. Publ.*, *229*, 9–20.

Lawrence, K. T., et al. (2006), Evolution of the eastern tropical Pacific through Plio-Pleistocene glaciation, *Science*, *312*, 79–83, doi:10.1126/science.1120395.

Lea, D. W. (2004), The 100 000-yr cycle in tropical SST, greenhouse forcing, and climate sensitivity, *J. Clim.*, *17*, 2170–2179, doi:10.1175/1520-0442(2004)017<2170:TYCITS>2.0.CO;2.

Lea, D. W., et al. (2000), Climate impact of late Quaternary equatorial Pacific sea temperature variations, *Science*, *289*, 1719–1724, doi:10.1126/science.289.5485.1719.

Lisiecki, L. E., and M. E. Raymo (2005), A Pliocene-Pleistocene stack of 57 globally distributed benthic $\delta^{18}O$ records, *Paleoceanography*, *20*, PA1003, doi:10.1029/2004PA001071.

Liu, Z., and T. D. Herbert (2004), High-latitude influence on the eastern equatorial Pacific climate in the early Pleistocene epoch, *Nature*, *427*, 720–723, doi:10.1038/nature02338.

Lunt, D. J., et al. (2008), Late Pliocene Greenland glaciation controlled by a decline in atmospheric CO_2 levels, *Nature*, *454*, 1102–1106, doi:10.1038/nature07223.

Maslin, M. A., et al. (1998), The contribution of orbital forcing to the progressive intensification of Northern Hemisphere glaciation, *Quat. Sci. Rev.*, *17*, 411–426, doi:10.1016/S0277-3791(97)00047-4.

Medina-Elizalde, M., and D. W. Lea (2005), The mid-Pleistocene transition in the tropical Pacific, *Science*, *310*, 1009–1012, doi:10.1126/science.1115933.

Medina-Elizalde, M., et al. (2008), Implications of seawater Mg/Ca variability for Plio-Pleistocene tropical climate reconstruction, *Earth Planet. Sci. Lett.*, *269*, 584–594.

Molnar, P., and M. A. Cane (2002), El Niño's tropical climate and teleconnections as a blueprint for pre–Ice Age climates, *Paleoceanography*, *17*(2), 1021, doi:10.1029/2001PA000663.

Newell, R. E. (1979), Climate and the ocean, *Am. Sci.*, *67*, 405–416.

Paillard, D., L. Labeyrie, and P. Yiou (1996), Macintosh program performs time-series analysis, *Eos Trans. AGU*, *77*, 379, doi:10.1029/96EO00259.

Philander, S. G., and A. V. Fedorov (2003), Role of tropics in changing the response to Milankovitch forcing some three million years ago, *Paleoceanography*, *18*(2), 1045, doi:10.1029/2002PA000837.

Pierrehumbert, R. T. (2000), Climate change and the tropical Pacific: The sleeping dragon wakes, *Proc. Natl. Acad. Sci. U. S. A.*, *97*, 1355–1358, doi:10.1073/pnas.97.4.1355.

Pisias, N. G., L. A. Mayer, and A. C. Mix (1995), Paleoceanography of the eastern equatorial Pacific during the Neogene: Synthesis of Leg 138 drilling results, *Proc. Ocean Drill. Program Sci. Results*, *138*, 5–21, doi:10.2973/odp.proc.sr.138.101.1995.

Ravelo, C. A., et al. (2004), Regional climate shifts caused by gradual global cooling in the Pliocene epoch, *Nature*, *429*, 263–267, doi:10.1038/nature02567.

Ravelo, C. A., et al. (2006), Evidence for El Niño–like conditions during the Pliocene, *GSA Today*, *16*, 1–11.

Raymo, M. E., and K. Nisancioglu (2003), The 41 kyr world: Milankovitch's other unsolved mystery, *Paleoceanography*, *18*(1), 1011, doi:10.1029/2002PA000791.

Raymo, M. E., W. F. Ruddiman, J. Backman, B. M. Clement, and D. G. Martinson (1989), Late Pliocene variation in Northern Hemisphere ice sheets and North Atlantic Deep Water circulation, *Paleoceanography*, *4*, 413–446, doi:10.1029/PA004i004p00413.

Raymo, M. E., et al. (1996), Mid-Pliocene warmth: Stronger greenhouse and stronger conveyor, *Mar. Micropaleontol.*, *27*, 313–326, doi:10.1016/0377-8398(95)00048-8.

Rickaby, R. E. M., and P. Halloran (2005), Cool La Niña during the warmth of the Pliocene?, *Science*, *307*, 1948–1952, doi:10.1126/science.1104666.

Seager, R., S. E. Zebiak, and M. A. Cane (1988), A model of the tropical Pacific sea surface temperature climatology, *J. Geophys. Res.*, *93*, 1265–1280, doi:10.1029/JC093iC02p01265.

Shackleton, N. J. (2000), The 100,000-year ice-age cycle identified and found to lag temperature, carbon dioxide, and orbital eccentricity, *Science*, *289*, 1897–1902, doi:10.1126/science.289.5486.1897.

Shackleton, N. J., et al. (1984), Oxygen isotope calibration of the onset of ice-rafting and history of glaciation in the northeast Atlantic, *Nature*, *307*, 620–623, doi:10.1038/307620a0.

Toggweiler, J. R. (2008), Origin of the 100,000-year timescale in Antarctic temperatures and atmospheric CO_2, *Paleoceanography*, *23*, PA2211, doi:10.1029/2006PA001405.

Vecchi, G. A., and J. B. Soden (2007), Global warming and the weakening of the tropical circulation, *J. Clim.*, *20*, 4316–4340, doi:10.1175/JCLI4258.1.

Vecchi, G. A., A. Clement, and B. J. Soden (2008), Examining the tropical Pacific's response to global warming, *Eos Trans. AGU*, *89*, 81, doi:10.1029/2008EO090002.

Wara, M. W., A. C. Ravelo, and M. L. Delaney (2005), Permanent El Niño–like conditions during the Pliocene warm period, *Science*, *309*, 758–761, doi:10.1126/science.1112596.

Wunsch, C., and P. Heimbach (2008), How long to oceanic tracer and proxy equilibrium?, *Quat. Sci. Rev.*, *27*, 637–651, doi:10.1016/j.quascirev.2008.01.006.

D. W. Lea, Department of Earth Science, University of California, Santa Barbara, CA 93106-9630, USA. (lea@geol.ucsb.edu)

M. Medina-Elizalde, Department of Geosciences, University of Massachusetts Amherst, Amherst, MA 01003, USA. (mmedina@geo.umass.edu)